

Swing excitation of magnetic fields in trailing spiral galaxies?

R. Rohde, G. Rüdiger, and D. Elstner

Astrofysikalisches Institut Potsdam, An der Sternwarte 16, D-14482 Potsdam, Germany

Received 10 December 1998 / Accepted 19 May 1999

Abstract. Swing-excited dynamo-induced magnetic fields in spiral galaxies are studied. We investigate the phenomenon of swing excitation with linear and nonlinear 3D numerical simulations of the galactic dynamo. The model includes differential rotation, axisymmetric and isotropic α -effect and uniform eddy diffusivity. The nonaxisymmetry is introduced via large-scale radial and azimuthal velocity components associated with a spiral density-wave perturbation.

In a first step we present a linear analysis in order to get insight in basic properties of the swing-excitation phenomenon. Both one and two-armed spiral galaxies are investigated. We find enlarged growth rates for the magnetic energy connected with the parametric resonance condition $\Omega_p \approx 2\omega_m$ (Ω_p pattern speed, ω_m magnetic drift rate), but only if the amplitude of the perturbation exceeds 10 km s^{-1} . The resonance behavior also appears in the nonlinear regime. The solutions are a mixture of several magnetic field modes. For a two-armed spiral the even modes ($m = 0, 2, \dots$) are preferred. The contribution of higher magnetic field modes to the solution is largest if the parametric resonance condition is fulfilled. The field geometry depends strongly on the pattern speed Ω_p , the excitation is weakest at the radius where the differentially rotating gas and the spiral pattern are corotating.

Key words: turbulence – ISM: magnetic fields – galaxies: ISM – galaxies: magnetic fields – galaxies: spiral

1. Introduction

Dynamo-induced nonaxisymmetric magnetic field modes in galactic disks exhibit a characteristic drift velocity in azimuthal direction, i.e. at a fixed location the magnetic field appears oscillating. The question arises whether and how the rotating spiral pattern interacts with these time-dependent and nonaxisymmetric magnetic field modes. In this context the phenomenon of swing excitation of galactic magnetic fields is discussed in the literature for years. Besides other effects as the influence of galactic encounters or contrast structures (for survey see Beck et al. 1996), the parametric resonance is investigated mostly

in order to explain bisymmetric field geometries as observed in M81 (Krause et al. 1989) or also in M 51, whose magnetic field can approximately be described as a superposition of field modes $m = 0$ and 1 (Berkhuijsen et al. 1997).

The origin of the galactic spiral structure is assumed to be due to a density wave in the disk leading to a time-dependent large-scale velocity field of the material and/or a time-dependent modulation of the α -coefficient.

Chiba & Tosa (1990), Chiba (1991) and Hanasz et al. (1991) discuss a resonance-like amplified growth rate of magnetic field energy in linear models with time-dependent large-scale velocity fields. Their approaches deal with analytical and numerical investigations of the simplified dynamo equation, which in its structure is believed to be comparable to the Mathieu equation in pendulum theory due to parametric resonances (Landau & Lifschitz 1969). These early models include several assumptions and approximations. Spatial derivations are reduced, the dynamo is treated locally in Cartesian geometry or only axisymmetric oscillations are discussed. The results strongly depend on the initial phase between the density wave and the dynamo wave. This property is criticized by Schmitt & Rüdiger (1992) who deal with solutions of a zero-dimensional model associated with a complex Mathieu-like equation. Swing excitation is found for appropriate ratios between radial and azimuthal velocity components. There is no dependency on the initial phase relation and the resonance condition $\Omega_p = 2\omega_m$ got lost. Hanasz & Chiba (1994) apply a multiple time-scale method to the models of Chiba & Tosa (1990). The swing excitation phenomenon is now found to be independent of the initial phase relation and restricted to the resonance condition $\Omega_p = 2\omega_m$.

A resonance-like behavior is also achieved for time-dependent modulation of the α -effect (Chiba 1991; Mestel & Subramanian 1991; Subramanian & Mestel 1993). Kuzanyan & Sokoloff (1993) point out in their linear analysis that the amplification of growth rates due to parametric resonance is proportional to the aspect ratio H/R of the disk. Since the aspect ratio is small for galaxies, the effect of parametric resonance should be too weak to explain bisymmetric magnetic fields in galaxies.

Moss (1996, 1997) re-investigates the effect of parametric resonance numerically for linear two-dimensional models including a nonaxisymmetric spiral pattern flow to the induction equation. An enlarged growth rate of the isolated $m = 1$ magnetic

field mode due to the modulated α -effect is found for fulfilled resonance condition. In Moss (1996) a resonance-like behavior is described also for noncircular velocities.

The simulations reported in Moss (1998) are for nonlinear 2D models, that are performed in order to investigate the appearance of interarm magnetic fields. These calculations also touch the occurrence of parametric resonances. It does not make much sense to discuss growth rates in nonlinear calculations, but for certain pattern speeds Ω_p the contribution of $m = 1$ and $m = 2$ modes to the magnetic field energy is found to be enlarged.

All these papers have accepted strong simplifications of the induction equation such as reducing the number of spatial dimensions, neglecting magnetic feedback or investigating isolated field modes as artificial initial conditions. It is thus our aim to find out, how the phenomenon of swing excitation occurs – if at all – in a rather realistic fully 3D nonaxisymmetric model of a spiral galaxy with nonlinear magnetic feedback included (α -quenching). The nonaxisymmetry is introduced via the large-scale velocity field modulated by a density-wave disturbance. For many galaxies it is not possible to clear up whether they lead or trail. But it is deduced as a general rule from unambiguous cases that spiral arms in galaxies are trailing (Binney & Tremaine 1987). Therefore we restrict ourselves to this type of one- and two-armed spiral galaxies.

Our 3D time-stepping code uses cylindrical polar coordinates with a resolution of 61 grid-points for each direction. The code in more detail is described in Elstner et al. (1990) and Rohde et al. (1998).

In Sects. 2 and 3 we present the configuration of our model. The results of the simulations are given in Sects. 4 and 5. There we discuss at first basic properties of the *axially symmetric* model such as critical dynamo numbers and azimuthal drift velocities of nonaxisymmetric magnetic field modes. In Sect. 4 we investigate the resonance behaviour of the *nonaxisymmetric* model in a *linear* analysis. The nonaxisymmetry is introduced via radial-azimuthal large-scale gas velocities. One-armed and two-armed spiral galaxies are taken into account. In Sect. 5 we finally present *nonlinear* calculations of the resonance behavior of a two-armed spiral galaxy model.

2. The mean-field electrodynamics

The evolution of the mean magnetic field $\langle \mathbf{B} \rangle$ is governed by the dynamo equation

$$\frac{\partial \langle \mathbf{B} \rangle}{\partial t} = \text{rot} (\langle \mathbf{u} \rangle \times \langle \mathbf{B} \rangle + \mathcal{E}), \quad (1)$$

where \mathcal{E} is the turbulent electromotive force, $\mathcal{E} = \langle \mathbf{u}' \times \mathbf{B}' \rangle$, and $\langle \mathbf{u} \rangle = (u_r, V + u_\phi, u_z)$ the large-scale velocity of the differentially rotating interstellar gas (Krause & Rädler 1980).

As usual, approximate scale-separation is adopted and we write

$$\mathcal{E}_i = \alpha_{ij} \langle B_k \rangle + \eta_{ijk} \langle B_j \rangle_{,k} \dots \quad (2)$$

In simplified models we assume the α -tensor as being isotropic with only diagonal terms of the form

$$\alpha_{ii} = \begin{cases} \alpha z(H^2 - z^2) & \text{for } |z| \leq H \\ 0 & \text{for } |z| > H \end{cases} \quad (3)$$

(no summation over i). The most important property of our model is the excitation of nonaxisymmetric field modes ($m \geq 1$). Since this is guaranteed by the choice of suitable parameters we do not discuss here the influence of anisotropic α -effect although this would be rather suitable for galactic dynamos (Schultz et al. 1994). Note that the α -tensor is axially symmetric and positive in the northern hemisphere.

For the eddy diffusivity η_T the rather large value $\eta_T = 10^{27} \text{ cm}^2 \text{ s}^{-1}$ is adopted corresponding to the thickness of the galaxy model in order to achieve nonlinear solutions saturating after reasonable times < 10 Gyr. Our value of η_T resembles the values calculated by Ferrière (1998) for several regions within the Galaxy due to the influence of super-bubbles. Note that within the meaning of a normalization a model with reduced length scales and diffusivity or with reduced gas velocities, alpha and diffusivity would lead to equivalent solutions in a different time scale.

3. The model

We consider galaxies to be differentially rotating turbulent disks embedded in a plasma of given conductivity. In the simplest case the “plasma” is vacuum and the conductivity therefore vanishes. The half-thickness of the galaxy is $H = 1.5$ kpc, its radius is $R_{\text{max}} = 15$ kpc.

The differential rotation is described by a Brandt-type law with $n = 2$ and $r_\Omega = 3$ kpc,

$$V = r\Omega = r\Omega_0 \left(1 + \left(\frac{r}{r_\Omega} \right)^n \right)^{-1/n} \quad (4)$$

(Donner & Brandenburg 1990; Sofue 1996). The velocity $V_\infty = r_\Omega \Omega_0$ is 180 km s^{-1} .

The generation of magnetic field in our model is described by the dynamo numbers characterizing both the induction effects with

$$C_\Omega = \frac{\Omega_0 H^2}{\eta_T} = 41.85, \quad C_\alpha = \frac{\alpha_{\text{max}} H}{\eta_T} = 4.65. \quad (5)$$

These values represent a galactic dynamo working in the $\alpha\Omega$ -regime¹. The value of C_α is high enough, so that also non-axisymmetric magnetic field modes are excited. Their possible swing excitation can therefore be investigated, although the axisymmetric field mode is the preferred one. The magnetic pitch angles are expected to have values around -20° estimated by $\Psi \approx -(C_\alpha/C_\Omega)^{1/2}$ after Beck et al. (1996).

The galactic spiral arms are introduced via an additional nonaxisymmetric velocity field based on the density-wave

¹ For a discussion of different dynamo regimes see Elstner et al. (1996).

Table 1. Critical dynamo numbers C_α^{crit} , growth rates γ of magnetic energy and drift velocities ω_m of the magnetic field modes $m = 0, 1, 2$ in a model with axially symmetric velocity field

m	C_α^{crit}	γ [Gyr^{-1}]	ω_m [Gyr^{-1}]
0	0.2	3.58	–
1	2.5	2.14	13.6
2	3.6	1.24	13.0

theory (Rohlfis 1977; Binney & Tremaine 1987). Its components are

$$\begin{aligned} u_r &= \chi u_0 \cos\left(m_p(\phi - \Omega_p t) + K \frac{r}{R_{\text{max}}}\right) f(r), \\ u_\phi &= u_0 \sin\left(m_p(\phi - \Omega_p t) + K \frac{r}{R_{\text{max}}}\right) f(r) \end{aligned} \quad (6)$$

with $m_p = 1, 2$ for a one and two-armed spiral galaxy, respectively. Azimuthal and radial flows are 90° out of phase as required by the theory. The frequency Ω_p gives the drift velocity of the spiral flow pattern, K its radial wave number. The factor $f(r) = (1 - r/R_{\text{max}})r/R_{\text{max}}$ is introduced in order to suppress the additional radial-azimuthal flow field at maximal radius and at $r = 0$. The ratio

$$\chi = \frac{\hat{u}_r}{\hat{u}_\phi} \quad (7)$$

is given in density wave theory as $\chi = -2\Omega(\Omega_p - m\Omega)/\kappa^2$ (with κ^2 epicycle frequency), χ should be negative. With a positive radial wave number K trailing spirals are described. The velocity u_0 may be of order 10 km s^{-1} .

In a trailing spiral the regions with radial velocities directed inwards are associated with the spiral arms (enhanced density). The azimuthal velocity is enlarged at the outer edge of the arms.

4. Growth rates and magnetic field drift

In all our simulations a combination of field modes $m = 0 \dots 5$ is taken as seed field. We define the fraction between the energy of one mode m and the total magnetic energy as

$$\epsilon_m = \frac{E_m}{E_{\text{total}}} = \frac{E_m}{E_0 + E_1 + \dots} \quad (8)$$

In a model with axially symmetric velocity field the energy of the mode $m = 0$ is dominant since it grows much faster than the other modes ($\epsilon_0 = 1$ after some time).

The parameters (5) fix a model that is supercritical for several magnetic field modes. The marginal (or critical) dynamo numbers for $m = 0, 1, 2$ for a model with axially symmetric velocity field are calculated in a linear analysis.

The linear analysis gives the growth rates γ of the magnetic field energy, $E \propto e^{2\gamma t}$. The magnetic field for modes $m \geq 1$ exhibits a characteristic drift velocity ω_m in azimuthal direction. For $m = 1$ and 2 the drift velocities are almost equal (cf. Table 1).

The phenomenon of swing excitation is studied by tuning the pattern speed Ω_p of the large-scale velocity field (6).

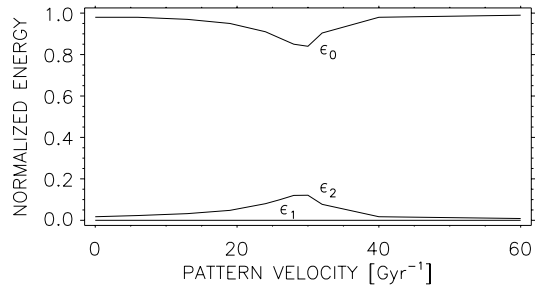


Fig. 1. Two-armed spiral galaxy: Normalized magnetic energy ϵ_0, ϵ_1 and ϵ_2 for magnetic field modes $m = 0, 1, 2$ after Eq. (8). The amplitude of the nonaxisymmetric velocity field is $u_0 = 20 \text{ km s}^{-1}$. The contribution of mode $m = 2$ is maximal for $\Omega_p \approx 2\omega_m$ (resonance condition)

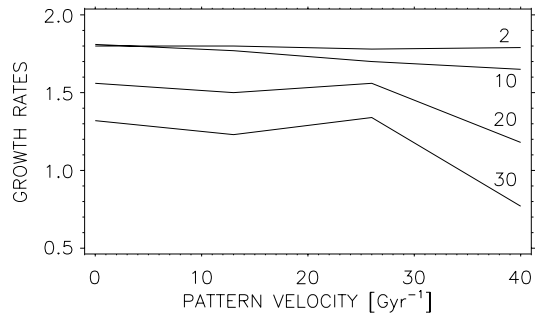


Fig. 2. Two-armed spiral galaxy: Linear growth rates γ of magnetic field energy for nonaxisymmetric velocities $u_0 = 2, 10, 20$ and 30 km s^{-1} . A weak maximum of the growth rates only appears for larger perturbations ($u_0 > 10 \text{ km s}^{-1}$) at $\Omega_p \approx 2\omega_m$

4.1. Two-armed spiral galaxies

Simulations with a two-armed nonaxisymmetric velocity field ($m_p = 2$; $K = 2\pi$; $u_0 = 20 \text{ km s}^{-1}$; $\chi = -1$) leads to more complicated situations. The final solution is not longer a single mode. It is thus not appropriate to discuss only isolated magnetic field modes. The solution can be described as a mixture of several modes, but in a two-armed spiral galaxy only the even modes contribute.

We only find for the magnetic field mode $m = 2$ a resonance-like behavior: In the model with pattern speed $\Omega_p = 26 \text{ Gyr}^{-1}$ the energy of the $m = 2$ magnetic field mode reaches its maximal value (Fig. 1). The pattern speed fulfills the parametric resonance condition ($\Omega_p \approx 2\omega_m$).

A weak maximum at pattern speed $\Omega_p \approx 26 \text{ Gyr}^{-1}$ also appears for the linear growth rates γ (Fig. 2, $u_0 = 20$ and 30 km s^{-1}). The growth rates for all pattern speeds Ω_p are smaller than the growth rate of the $m = 0$ mode in the unperturbed (axially symmetric) model – but larger than the unperturbed $m = 2$ growth rate.

The maximal growth rate (Fig. 2) and the contribution of the magnetic $m = 2$ mode (Fig. 3) depend on the strength of the nonaxisymmetric velocity field. There is no maximum for small nonaxisymmetric velocity amplitudes (here $u_0 = 2 \text{ km s}^{-1}$, $u_0 = 10 \text{ km s}^{-1}$).

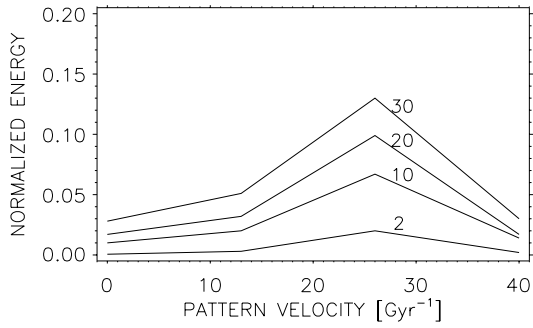


Fig. 3. Two-armed spiral galaxy: Contributions of normalized $m = 2$ magnetic field energy $\epsilon_2 = E_2/E_{\text{total}}$ for nonaxisymmetric velocities $u_0 = 2, 10, 20$ and 30 km s^{-1}

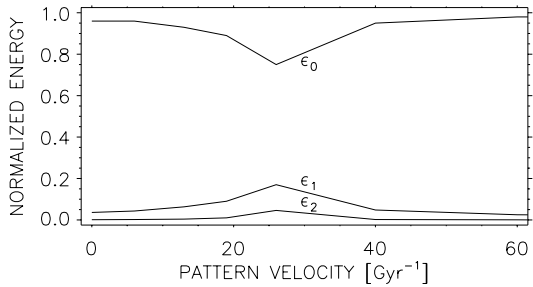


Fig. 4. One-armed spiral galaxy: Normalized magnetic energy ϵ_0, ϵ_1 and ϵ_2 for magnetic field modes $m = 0, 1, 2$; $u_0 = 20 \text{ km s}^{-1}$. The contribution of mode $m = 1$ is maximal for $\Omega_p \approx 2\omega_m$ (resonance condition)

The influence of the nonaxisymmetry vanishes for very fast rotating pattern. With an (unrealistic) pattern speed of 100 Gyr^{-1} we again achieve a solution very close to the axially symmetric model. Note that in this case the corotation radius between the spiral pattern and the differentially rotating interstellar gas is outside the computational domain.

4.2. One-armed spiral galaxies

A resonance-like behavior of the $m = 1$ magnetic field can however be found for a one-armed spiral galaxy² (Figs. 4 and 5). A trailing spiral ($m_p = 1, K = \pi$) may be defined with $\chi = -1$ and $u_0 = 20 \text{ km s}^{-1}$. The phenomenon is equivalent to the contribution of the $m = 2$ magnetic field in a two-armed spiral galaxy; but the excitation is now stronger - an effect due to the fact, that the critical dynamo number for the mode $m = 1$ is smaller than that for the mode $m = 2$.

5. The nonlinear regime

The 3D nonlinear model is based on the standard α -quenching mechanism

$$\alpha = \frac{\alpha_0}{1 + B^2} \quad (9)$$

² An example for an one-armed spiral galaxy is NGC4378 (cf. Byrd et al. 1994).

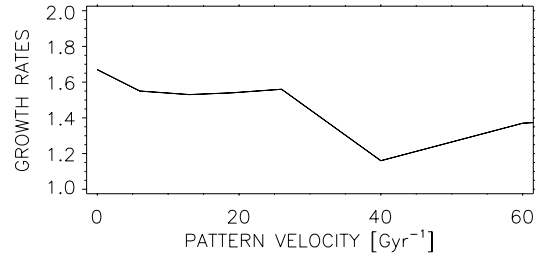


Fig. 5. One-armed spiral galaxy: Linear growth rates γ of magnetic field energy for several pattern speeds Ω_p ; $u_0 = 20 \text{ km s}^{-1}$. A weak maximum arises for $\Omega_p \approx 2\omega_m$ (resonance condition)

with B normalized with the equipartition field. The model parameters are the same as for the linear analysis of a two-armed spiral galaxy model. The seed field again is a combination of field modes $m = 0 \dots 5$.

The simulations show that basic properties of the linear analysis also exist here. There is a resonance-like maximal contribution of magnetic energy belonging to the mode $m = 2$ at pattern speed $\Omega_p \approx 26 \text{ Gyr}^{-1}$ ($\Omega_p \approx 2\omega_m$, Fig. 6). The $m = 1$ magnetic field mode again does *not* contribute to the final magnetic field configuration. It can be seen in Fig. 6 (solid lines) that the $m = 1$ contribution vanishes after about 2 Gyr.

The field geometry strongly depends on the velocity field pattern and is thus related to the corotation radius r_{co} , the radius where the pattern speed equals the galactic angular velocity. For small pattern speeds (r_{co} close to R_{max}) the field is concentrated in the inner parts of the galaxy (Figs. 7a and 8a). The magnetic arms are due to a field concentration into regions with negative radial velocity components. The situation changes for increased Ω_p . The magnetic field is then also excited at larger radii and mostly outside the corotation radius r_{co} (Figs. 7c and 8c). The field is shifted into regions with positive velocity components, i.e. the interarm region.

The sharpest field concentration arises in the model that fulfills $\Omega_p \approx 2\omega_m$. The region with maximal field follows the region with velocities directed inwards. These regions correspond to the inner edge of an optical spiral arm in which the radial velocities are directed towards the galactic center (Figs. 7b and 8b). This situation stands in between the ‘extreme’ cases with small and large pattern speed (large and small corotation radius, respectively) and finally includes the behavior of both. The field excitation is smallest in regions where the differentially rotating gas and the spiral pattern are corotating (Fig. 8).

The preferred contribution of higher azimuthal field modes (here $m = 2$) in case of resonance introduce magnetic arms in the large-scale magnetic field, which are correlated with the location of the corotation radius. This influence of the corotation radius onto the occurrence of magnetic arms is also discussed by Moss et al. (1999) for the barred galaxy IC4214 (‘corotation resonance’).

Figs. 9 and 10 show the magnetic pitch angle of the model with pattern speed 26 Gyr^{-1} at two different radii. The magnetic pitch angle reaches values of nearly -20° in regions with

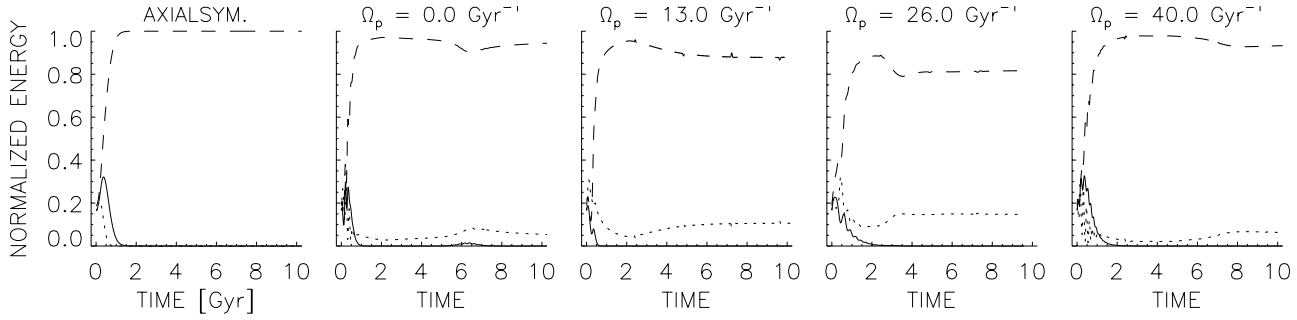


Fig. 6a–e Normalized magnetic energies $\epsilon_m = E_m/E_{\text{total}}$, $m = 0$ (dashed), 1 (solid), 2 (dotted) for magnetic field energy of several modes taken for several pattern speeds Ω_p of a two-armed spiral galaxy; $u_0 = 20 \text{ km s}^{-1}$. The contribution of the mode $m = 2$ reaches a maximal value for $\Omega_p = 26 \text{ Gyr}^{-1}$

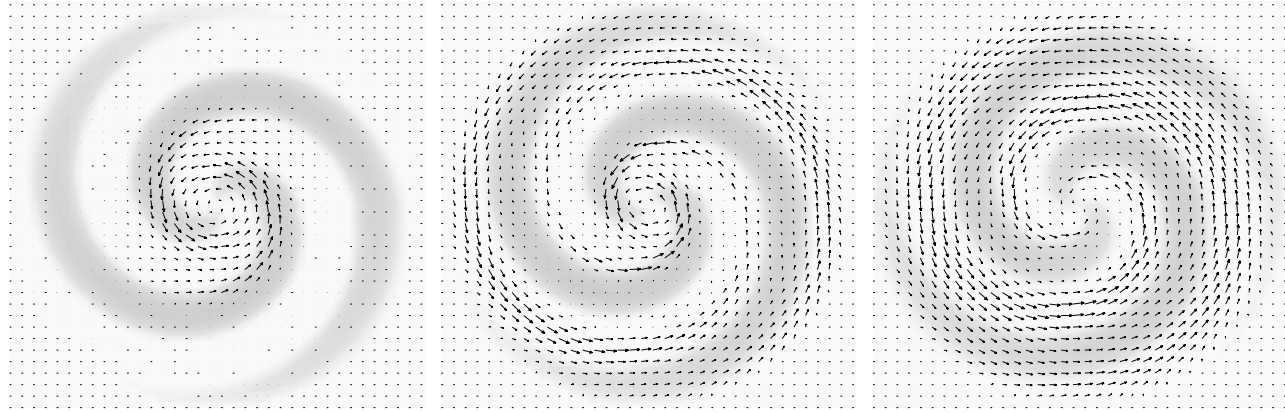


Fig. 7a–c. Magnetic field in the equatorial plane of a two-armed spiral galaxy model for different pattern speed $\Omega_p = 13$ (a), 26 (b) and 40 Gyr^{-1} (c); $u_0 = 20 \text{ km s}^{-1}$. Regions with radial velocity directed inwards (spiral arms) are shown in grey scale

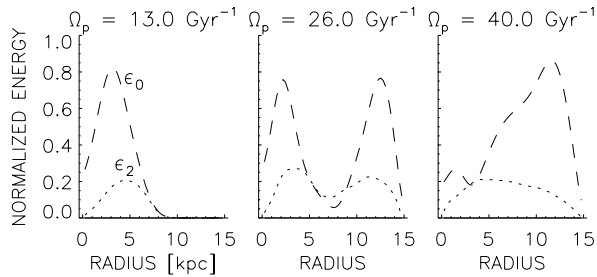


Fig. 8a–c. Normalized energy ϵ_m of mode $m = 0$ (dashed) and 2 (dotted) for the two-armed galaxy model; $u_0 = 20 \text{ km s}^{-1}$. The pattern speeds Ω_p define corotation radii $r_{\text{co}} = 13.5$ (a), 6.2 (b), 3.3 kpc (c). The field excitation is decreased near r_{co}

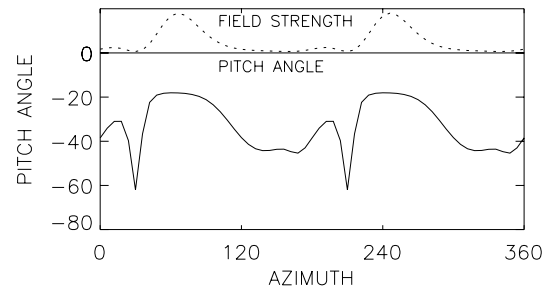


Fig. 9. Magnetic pitch angles (solid) compared with normalized magnetic field strength (dotted) at $r = 5 \text{ kpc}$ for the two-armed galaxy model with $\Omega_p = 26 \text{ Gyr}^{-1}$; galactic midplane; $u_0 = 20 \text{ km s}^{-1}$

substantial magnetic field, but it is remarkably larger in regions where the field is weak.

6. Conclusion

The basic result of our 3D linear and nonlinear simulations is the resonance-like contribution of higher magnetic field modes to the final solution if the resonance condition $\Omega_p \approx 2\omega_m$ is fulfilled (Figs. 1 and 4). The excitation of nonaxisymmetric field modes is increased in case of resonance. This behavior survives in the *nonlinear* regime (Fig. 6). It resembles the solutions for

the 2D nonlinear models described by Moss (1998), where most simulations indeed were based on a superposition of a one and two-armed spiral perturbation.

In all nonaxisymmetric models the resulting magnetic field is a mixture of several modes. For two-armed spirals only the even modes ($m = 0, 2, \dots$) are preferred but for one-armed spirals all modes contribute.

We also find a resonance maximum for the growth rates of magnetic energy from linear analysis (Fig. 2, $u_0 = 20$ and 30 km s^{-1}), whose appearance depends on the amplitude of the nonaxisymmetric velocity fields. The idea is supported that

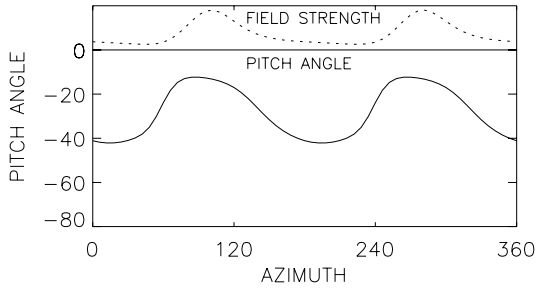


Fig. 10. The same as in Fig. 9 but for $r = 10$ kpc

swing excitations indeed may exist in spiral galaxies. But in the frame of our models the phenomenon is only weak since the maximum arises only for amplitudes larger than (the realistic value of) $u_0 = 10 \text{ km s}^{-1}$ (Fig. 2). For lower amplitudes higher magnetic field modes also weakly contribute to the solution (Fig. 3), but without resonance-like enlarged growth rate. We therefore conclude that in the nonlinear regime the effects would be very weak for smaller and more realistic amplitudes.

Acknowledgements. R.R. thanks the Deutsche Forschungsgemeinschaft for the support which made this work possible.

References

Beck R., Brandenburg A., Moss D., Shukurov A., Sokoloff D.D., 1996, *ARA&A* 34, 155
 Berkhuijsen E.M., Horellou C., Krause M., et al., 1997, *A&A* 318, 700

Binney J., Tremaine S., 1987, *Galactic Dynamics*. Princeton University Press, Princeton
 Byrd G., Freeman T., Howard S., 1994, *AJ* 108, 2078
 Chiba M., 1991, *MNRAS* 250, 769
 Chiba M., Tosa M., 1990, *MNRAS* 244, 714
 Donner K.J., Brandenburg A., 1990, *A&A* 240, 289
 Elstner D., Meinel R., Rüdiger G., 1990, *GAFD* 50, 85
 Elstner D., Rüdiger G., Schultz M., 1996, *A&A* 306, 740
 Ferrière K., 1998, *A&A* 335, 488
 Hanasz M., Chiba M., 1994, *MNRAS* 266, 545
 Hanasz M., Lesch H., Krause M., 1991, *A&A* 243, 381
 Krause F., Rädler K.-H., 1980, *Mean-field magnetohydrodynamics and dynamo theory*. Akademie-Verlag, Berlin
 Krause M., Beck R., Hummel E., 1989, *A&A* 217, 17
 Kuzanyan K.M., Sokoloff D.D., 1993, *Ap&SS* 208, 245
 Landau L.D., Lifschitz E.M., 1969, *Mechanics*. Pergamon Press, Oxford
 Mestel L., Subramanian K., 1991, *MNRAS* 248, 677
 Moss D., 1996, *A&A* 308, 381
 Moss D., 1997, *MNRAS* 289, 554
 Moss D., 1998, *MNRAS* 297, 860
 Moss D., Rautiainen P., Salo H., 1999, *MNRAS* 303, 125
 Rohde R., Elstner D., Rüdiger G., 1998, *A&A* 329, 911
 Rohlfs K., 1977, *Lectures on Density Wave Theory*. Lecture Notes in Physics 69, Springer, Berlin
 Schmitt D., Rüdiger G., 1992, *A&A* 264, 319
 Schultz M., Elstner D., Rüdiger G., 1994, *A&A* 286, 72
 Sofue Y., 1996, *ApJ* 458, 120
 Subramanian K., Mestel L., 1993, *MNRAS* 265, 649